RESEARCH ON HOT SPOT TEMPERATURE INVERSION METHOD OF OIL-IMMERSED TRANSFORMER BASED ON MULTI-PHYSICAL FIELD COUPLING OF MAGNETIC-THERMAL-FLUID

by

LingYun GU[a], FaTing YUAN[b,c*], NaiYue ZHANG[b], XueFeng BAI[a], Xin ZHANG[a], WenPeng GAO[a], Yan WU[a], and ZhiXin BAI[a]

[a]Beijing Key Laboratory of Distribution Transformer Energy-Saving Technology (China Electric Power Research Institute), Beijing, China
[b]College of Electrical Engineering and New Energy, China Three Gorges University, Yichang, China
[c]Hubei Provincial Engineering Technology Research Center for Power Transmission Line, China Three Gorges University, Yichang, China

Original scientific paper
https://doi.org/10.2298/TSCI240330172G

The hot spot temperature is an important factor affecting the operation state and insulation life of oil-immersed transformer. It is of great value to carry out multi-physical field coupling simulation research on magnetic-fluid-thermal field of oil-immersed transformer and accurately calculate and predict the hot spot temperature of transformer for transformer service life evaluation. In this paper, the oil immersed transformer is taken as the research object, and five characteristic parameters of the hysteresis model are obtained by using PSO algorithm according to the experimental magnetic characteristics data of the core material and the classical Jiles-Atherton (J-A) hysteresis model, A 3-D simulation model of magnetic-fluid-thermal field is established based on the electrical and structural parameters of the oil-immersed transformer. Combined with the magnetic characteristics of the core material, the thermal field and the surrounding fluid distribution of the transformer core and winding are obtained by two-way coupling method. On this basis, in order to accurately reflect the correlation between the hot spot temperature of the transformer winding and the temperature of the oil tank wall, the selection position of the characteristic temperature point of the transformer tank wall is determined by streamline analysis method, and the hot spot temperature of the oil-immersed transformer is retrieved by support vector machine method. The results show that the prediction accuracy of the hot spot temperature reaches 0.998, and the inversion method has a high enough accuracy. It provides theoretical basis and technical support for real-time monitoring of hot spot temperature in oil-immersed transformer windings.

Key words*: hot spot temperature, PSO algorithm, support vector machine, oil-immersed transformer*

Introduction

As the key equipment of distribution system, the oil-immersed transformer plays an important role in voltage conversion and power distribution. In recent years, with the rapid

*Corresponding author, e-mail: yuanfatinghss@163.com

development of China's economy, in order to meet the growing demand for power supply, the scale of China's power grid is expanding year by year, and the voltage level is also constantly improving. Transformer, as an important equipment in power system, plays a key role in voltage transformation, power distribution and transfer. The stable and safe operation of transformer is very important to the safe and reliable operation of power grid. The oil-immersed transformer with transformer oil as insulating medium has the advantages of good heat dissipation, low loss, large capacity and reliable operation, so it is widely used in power system. In the actual operation process, thermal aging of transformer is the most important factor that causes its service life to decrease. Therefore, the accurate calculation and optimization of transformer hot spot temperature is of great engineering value for transformer operation reliability analysis and service life evaluation.

The parameter identification methods of J-A model mainly include formula method and fitting method. The formula method mainly determines the parameters of J-A model through the iterative calculation of the key parameters of hysteresis curve. Liu *et al.* [1] used the formula method to identify parameters of the measured magnetization curve, but the identification results were greatly affected by the initial iterative values. Aiming at the difficulty of parameter determination in the J-A model describing the hysteresis characteristics of iron cores, Li *et al*. [2] proposed a parameters-by-parameter optimization algorithm, which is simple and highly accurate. Wilson *et al.* [3] used genetic algorithm to extract the optimal parameters of J-A hysteresis model, and compared the parameter identification results of simulated annealing algorithm, the results showed that the identification results of genetic algorithm were more accurate. Cao *et al*. [4] proposed an improved particle swarm optimization (PSO) algorithm to identify key parameters in the J-A hysteresis model. Compared with the parameter identification results of other intelligent algorithms, the error between the hysteresis loop obtained by the improved algorithm and the measured hysteresis loop is minimal, and the identification efficiency is high. Therefore, the fitting method is used to identify the parameters of J-A hysteresis model, which lays a foundation for the subsequent calculation of core loss.

In order to accurately simulate the temperature rise distribution of the transformer, it is necessary to accurately calculate the loss of the transformer. In the process of transformer operation, the loss mainly includes the core loss caused by the magnetic flux passing through the core and the winding loss caused by the current flowing through the winding. In addition, eddy current losses caused by leakage flux are also included, and these losses will be diffused outward in the form of heat, causing the temperature of each transformer component to rise [5]. Therefore, the accurate calculation of the loss of oil-immersed transformer is very important to study the distribution of transformer thermal field. Wakil *et al*. [6] conducted 2-D numerical simulation of different transformer oil passage structures and oil flow velocities, studied the change of oil flow velocity and temperature rise distribution in transformer oil passage, and optimized transformer cooling based on the calculation results. Ostrenko *et al*. [7] coupled IEM and FEM to calculate the stray loss and temperature rise distribution of the structural components of power transformers and reactors, and compared it with the experimental results to verify the accuracy of the method. Peker *et al*. [8] uses an integral transform, namely Kashuri Fundo transform, by blending with the homotopy perturbation method for the solution of nonlinear fractional porous media equation and time-fractional heat transfer equation with cubic non-linearity. Peker *et al*. [9] solves Abel's integral equation by Kashuri Fundo transform and some applications are made to explain the solution procedure of Abel's integral equation by Kashuri Fundo transform. Literature [10-13] considers Kashuri Fundo transform, an integral transformation, which is proved to be an effective method to solve steady-state heat transfer

problems. Pan *et al*. [14] simplified the winding structure and oil flow conditions, set the simulation parameters based on the existing technical parameters and monitoring data, and proposed a simulation analysis method for the hot spot temperature of large transformers based on the thermal field distribution calculation. By comparing the measured data, the calculation results of the standard model and the simulation results of the hot spot temperature of the top oil temperature of the transformer. The rationality and accuracy of the method are verified.

In this context, the classical J-A hysteresis model is used to accurately identify the characteristic parameters of iron core materials, and a multi-physical coupling numerical model of transformer fluid-thermal field is established to obtain and optimize the thermal field distribution of each transformer component. On the basis of reducing transformer hot spot temperature, the inversion model of transformer hot spot temperature is carried out. The research results provide theoretical support and method guidance for the rapid and accurate acquisition of transformer hot spot temperature and the reduction of transformer temperature rise, and realize the stable and safe operation of oil-immersed transformers in power system, which has certain academic value and important practical significance.

Identification of transformer characteristic parameters

The basic theory of Jiles-Atherton hysteresis model

The J-A model describes the relationship between magnetization and magnetic field strength, considering the principle of magnetic domain wall displacement and energy balance based on the magnetic domain theory, and better reflects the physical process of magnetization of magnetic materials. The physical meaning of the model is clear and the parameters are few, and it is widely used in the field of hysteresis modeling.

In the J-A model, the total magnetization, M, is expressed as the sum of reversible magnetization, M_{rev}, and irreversible magnetization, M_{irr}:

$$M = M_{\text{irr}} + M_{\text{rev}} \tag{1}$$

where M_{irr} is caused by the magnetic domain formed by the discontinuity of the material structure and M_{rev} is caused by the magnetic domain of the elastic mode. According to the physical mechanism of the process, the relationship between irreversible magnetization M_{irr} and reversible magnetization M_{rev} is:

$$M_{\text{rev}} = c\left(M_{\text{an}} - M_{\text{irr}}\right) \tag{2}$$

where M_{an} is the no hysteresis magnetization and is a reversible coefficient.

The inverse J-A hysteresis model is expressed as:

$$\frac{\mathrm{d}M}{\mathrm{d}B} = \frac{\delta\left(M_{\text{an}} - M\right) + ck\delta\dfrac{\mathrm{d}M_{\text{an}}}{\mathrm{d}H_e}}{\mu_0\left[(1-\alpha)\left(\delta\left(M_{\text{an}} - M\right) + ck\delta\dfrac{\mathrm{d}M_{\text{an}}}{\mathrm{d}H_e}\right) + k\delta\right]} \tag{3}$$

The J-A model feature parameter identification based on PSO algorithm

The PSO algorithm was proposed by American psychologist Kennedy and electrical engineer Eberhart in 1995. The core idea of the algorithm is to simulate the social and migration

behavior of birds during the foraging process [15]. Suppose a constant size flock of birds is hunting in an area where there is only one piece of food, and the flock does not have the exact location of the food, only the location of their companions and the distance between them and the food. The flock needs to keep searching in the direction of the companion closest to the food. In PSO, particles are regarded as birds, and each particle is constantly adjusted according to its own situation and that of other particles, so that the whole population is constantly closer to the optimal solution [16]. The PSO has the advantages of simple concept, simple iteration format and fast convergence speed, and has become a research hotspot of modern optimization methods. The flow chart of PSO algorithm is shown in fig. 1.

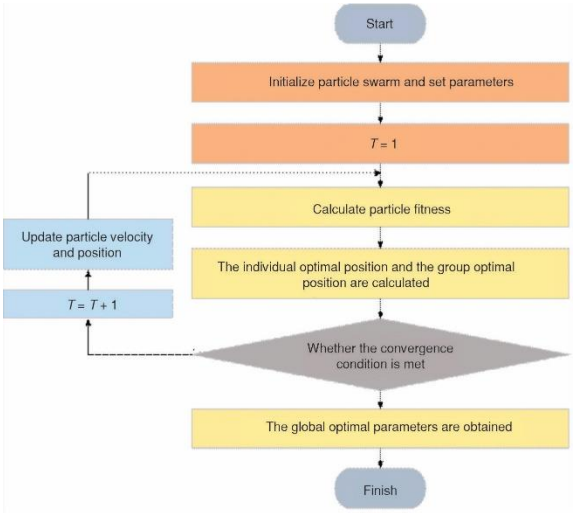

Figure 1. Flow chart of PSO algorithm

Parameter identification result

According to the J-A hysteresis model theory, a total of five parameters need to be identified. The measured values of hysteresis loops are used to identify material parameters, and the obtained parameter identification results are shown in tab. 1.

Table 1 Results of model parameter identification

Parameter	M_s	α	a	c	k	RMSE
Identification result	1802941	4.34×10^{-5}	17.41	0.209	35.37	2.557

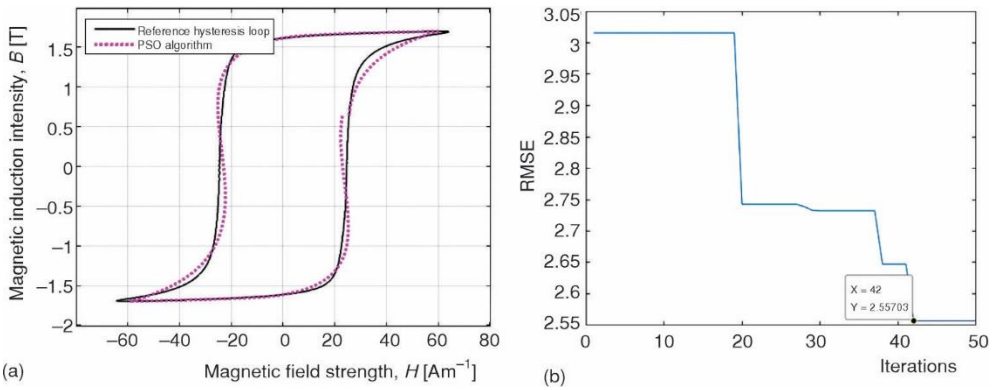

Figure 2. The PSO algorithm parameter fitting results and RMSE; (a) parameter fitting results and (b) RMSE

The obtained identification parameters were substituted into the model, and the comparison results between the J-A curve and the measured values of the parameters identified

based on the PSO algorithm and the changes of the root-mean-square error with the number of iterations were shown in fig. 2.

It can be seen from fig. 2 that the hysteresis loop fitted by the model parameters obtained by the PSO algorithm is not much different from the hysteresis loop measured by the experiment, and the fitting effect is relatively good. The PSO retains the global search strategy, but does not use the update method of crossover and variation similar to evolutionary algorithm, and keeps the population size constant during the search, so that it maintains a fast convergence rate. It can be seen from the figure that in parameter identification of J-A hysteresis model, the curve identified by PSO algorithm is in good agreement with the measured curve, which proves the practicability of the method.

Simulation calculation of transformer fluid-thermal field

Basic structure parameters and equivalent model of transformer

This paper takes an oil-immersed transformer as the research object. Oil-immersed transformer is mainly composed of winding, core and cooling system, cooling system includes transformer oil and heat sink. The established oil-immersed transformer model has a total of 54 heat sinks, including 19 on the front and 8 on the side. The length of each heat sink is 700 mm, the width is 80 mm and the thickness is 7 mm. The 3-D model diagram is shown in fig. 3. The rated voltage of the high and low voltage windings of the oil-immersed transformer is 20 kV and 400 V, respectively, the rated capacity is 200 kVA, and the rated operating frequency is 50 Hz. The inner core of the transformer is the main channel of magnetic flux, which is made of cold-rolled silicon steel sheet laminated. The winding is multi-layer cylindrical structure, the inner ring is low voltage winding, the outer ring is high voltage winding, and the conductor of the winding is enameled flat copper wire. The transformer oil tank is filled with transformer oil to play the role of insulation and heat dissipation. The relevant structural parameters of the oil-immersed transformer are shown in tab. 2.

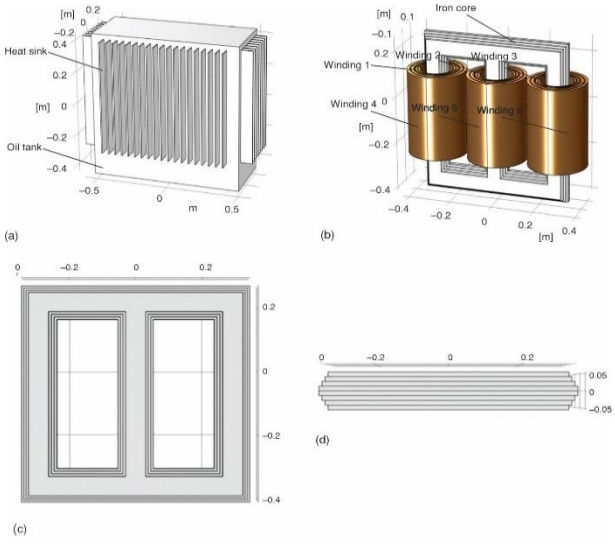

Figure 3. Oil immersed transformer 3-D model diagram; (a) external structure, (b) internal structure, (c) front view of core structure, and (d) top view of core structure

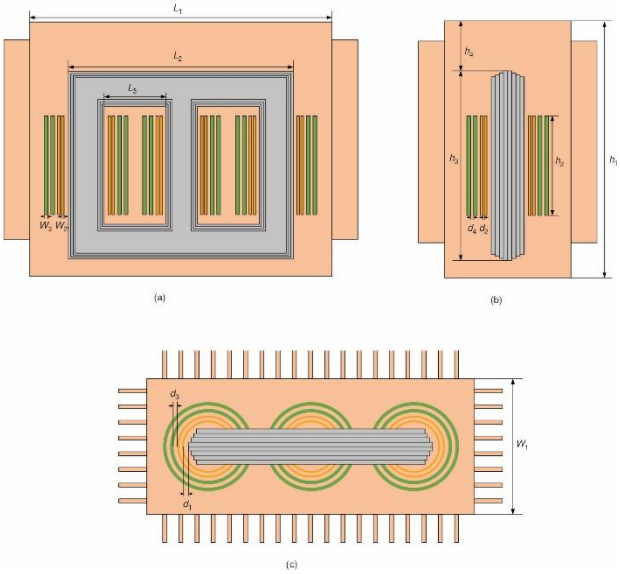

Figure 4. Oil-immersed transformer structure diagram; (a) front view, (b) side view, and (c) top view

The structure diagram of the oil-immersed transformer is shown in fig. 4.

Table 2. Structure parameters of oil-immersed transformer

Argument	Value [mm]	Argument	Value [mm]
L1	1020	W1	420
L2	680	W2	7.5
L3	182.5	W3	12
h1	900	d1	16
h2	360	d2	4
h3	680	d3	10
h4	180	d4	5

Heat transfer mechanism of transformer

In the actual operation of the transformer, the winding and core of the transformer produce loss, which is converted into heat energy. The outward diffusion process of heat generated by winding and core mainly includes heat conduction, convective heat transfer and heat radiation [17]. Heat is diffused from the inside of the winding and core to the surface of the winding and core by heat conduction, and the heat from the surface of the winding and core is diffused by heat conduction to the transformer oil near the winding and core. As the temperature of the transformer oil continues to rise, the density of the heated transformer oil continues to decrease, thus flowing upward. Heat from the transformer oil near the winding and core is diffused to the inner surface of the tank by convection heat transfer. Resulting in lower transformer oil temperature, transformer oil density increases, then it flows down the transformer, into the bottom of the transformer, re-flow around the winding to form a closed circulating oil circuit. At the same time, there is also thermal radiation between the winding and the core surface. The heat transfer mechanism of the oil-immersed transformer is shown in fig. 5.

Solving domain boundary conditions and grid testing

In the transformer simulation model, the core and winding losses are used as the heat source conditions for temperature field simulation, the ambient temperature at the model

boundary is set to 20 °C, the heat flux of the transformer shell is set to external natural convection, and the transformer oil is an incompressible Newtonian fluid. At the junction of transformer oil and oil tank wall, it is considered that the fluid near the wall is relatively stationary relative to the wall, that is, the relative velocity of the oil flow near the oil tank wall is zero.

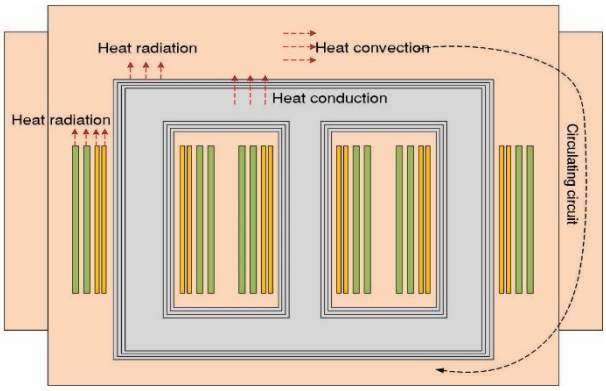

Figure 5. Schematic diagram of heat transfer mechanism of oil-immersed transformer

The boundary conditions are shown in fig. 6.

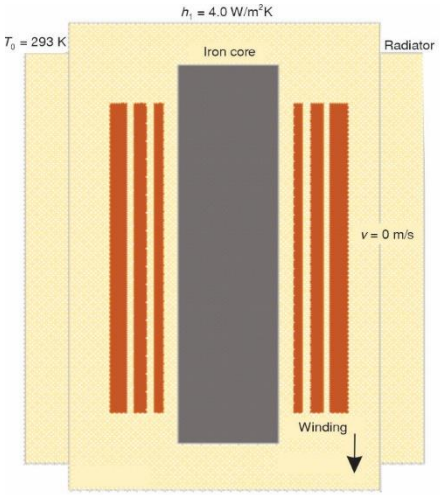

Figure 6. Boundary condition diagram

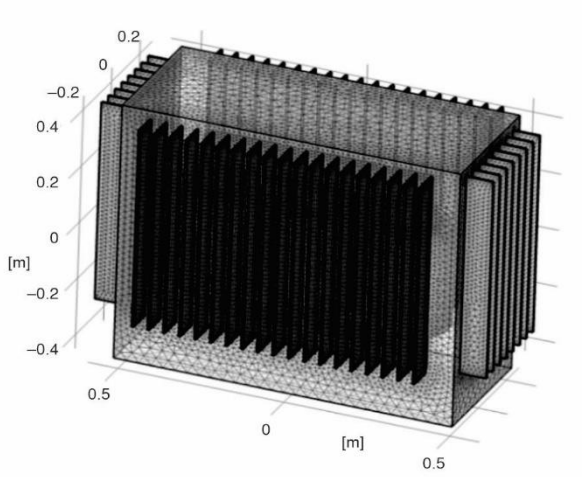

Figure 7. Fluid-thermal field simulation grid profile diagram

In order to take into account the speed and accuracy of the simulation calculation of fluid-thermal field, the grid near the core, winding and heat sink is dense, while the grid in other parts is thicker. The section of transformer fluid-thermal field simulation unit is shown in fig. 7. The model is divided into 894604 domain units, 648068 tetrahedral units, and 22076 edge units, and the number of grid fixed points is 249939.

Analysis of simulation results of transformer fluid-thermal field

According to the electrical and structural parameters of the oil-immersed transformer, the simulation model is established by using the finite element simulation software COMSOL

and the simulation calculation method of the fluid-thermal field. After setting the material parameters, heat sources, boundary conditions and grid division of the model, the thermal field simulation results are: fig. 8(a) shows the thermal field distribution diagram of the oil-immersed transformer at t = 15 hours, and it can be considered that its temperature reaches a stable state. The hot spot temperature of the transformer is 89.61 ℃, located in the area of the low voltage winding. Because the density of transformer oil becomes smaller after heating, the transformer oil with higher temperature will continue to move upward, and the temperature is higher at the upper end of the core and winding.

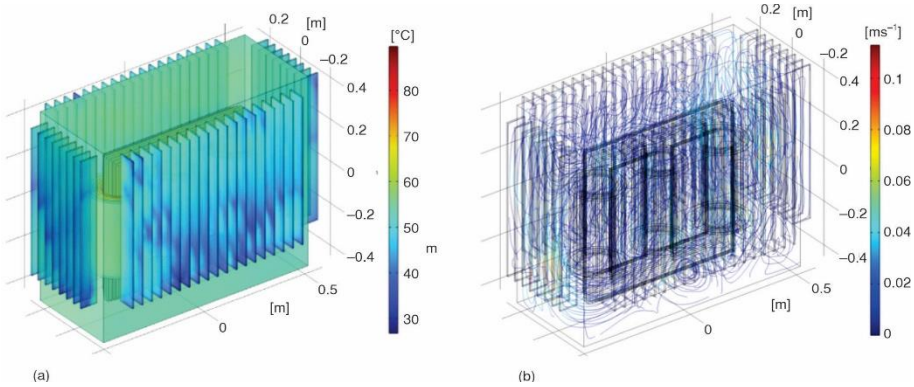

Figure 8. Distribution of transformer thermal field; (a) overall thermal field distribution of transformer and (b) thermal field distribution of transformer winding and core

The distribution of transformer fluid field is shown in fig. 8(b). From the flow rate distribution, it can be seen that the oil flow at the bottom of the transformer box flows to the top layer under the action of thermal floating lift after heating through the winding, and the transformer oil flowing to the top of the box will flow into the heat sink for cooling, and then flow to the bottom of the transformer box through the heat sink, so the cycle eventually forms the whole process of the oil flow heat dissipation inside the transformer. In order to study the distribution law of the thermal field inside the transformer, different paths of the transformer as shown in fig. 9 are selected, and the thermal field distribution obtained is shown in fig. 10.

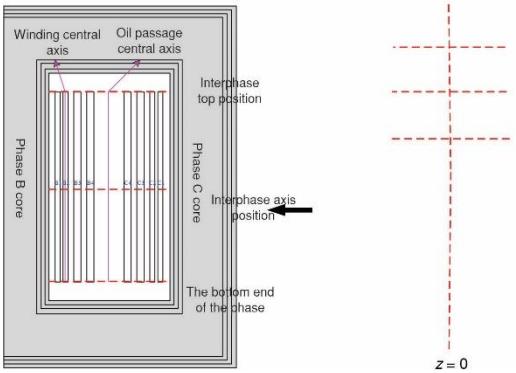

Figure 9. Transformer data extraction path

Figure 10 extracts the thermal field distribution at different planes of the transformer. As can be seen from the figure, the high temperature area of the transformer is mainly distributed in the winding part, which is because the low-voltage coil is located inside the winding, the heat production level is high and the heat dissipation capacity is poor. As the temperature of transformer oil increases and the density decreases, the hot transformer oil gradually rises and continuously convective heat transfer with the surrounding fluid. After the oil temperature drops, the density rises and flows back to the bottom of the transformer, resulting in the overall upper part of the transformer being higher than the lower part. The temperature distribution of the transformer along different paths is shown.

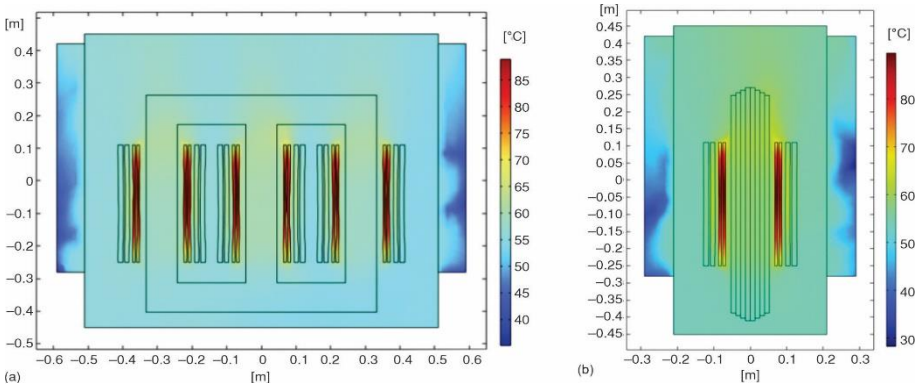

Figure 10. Thermal field distribution at different planes of transformer; (a) z = 0 plane thermal field distribution and (b) x = 0 plane thermal field distribution

Figure 11 extracts the temperature distribution of the transformer along different paths, extracts the temperature distribution of the low-voltage winding, high-voltage winding and the central axis between the two phases of the B and C phase transformer, and obtains the temperature distribution of the top, bottom and central axis of the winding between the B and C phases. As can be seen from the figure, the coil temperature of the axial winding increases first and then decreases, and the highest temperature is about 2/3 of the winding, and the temperature of the low-voltage winding is much higher than that of the high-voltage winding. The temperature distribution of each phase winding is basically the same, and the temperature of the B-phase winding is slightly higher than that of the C-phase winding, which is because the B-phase winding is located in the middle of the transformer oil tank and has poor heat dis-sipation capacity.

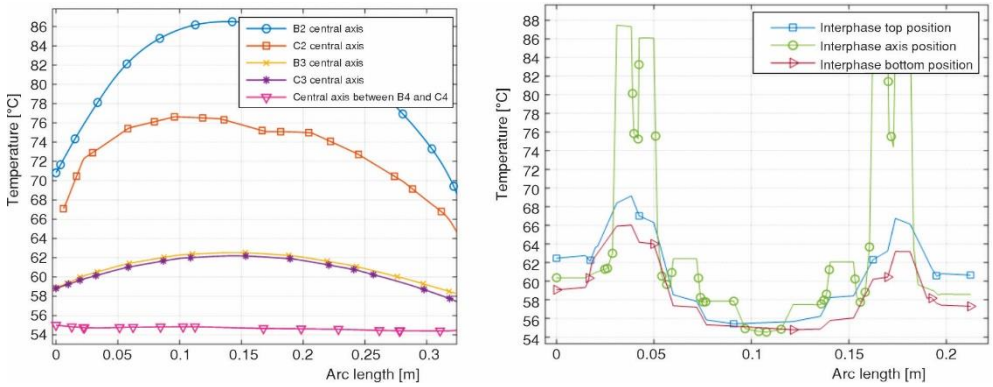

Figure 11. Temperature distribution of the transformer along different paths

The temperature distribution at the upper end of the radial upper winding is slightly higher than that at the lower end, and the temperature distribution trend of the two parts is consistent. The temperature along the radial central axis, however, is significantly higher than at both ends. This discrepancy arises due to the relatively smaller contact area between the central axis region and the transformer oil, and the heat dissipation capacity is poor.

Figure 12 extracts the fluid field distribution of the transformer along different paths. Figure12(a) shows the transformer oil fluid field distribution in the x = 0 plane, and fig.12(b) shows the transformer oil flow velocity diagram along different paths. It can be seen from the

figure that the flow velocity distribution trend at the central axis between different windings is basically the same, showing a phenomenon of fast flow velocity at both ends and slow flow velocity in the middle. The winding coil conducts heat to the surrounding transformer oil, and the heated transformer oil flows through the heat sink and the surrounding transformer oil convection heat transfer, and then flows back to the bottom of the transformer. Due to the slower flow velocity in the central region, heat accumulates at the intermediate position, leading to elevated temperatures in the upper part of the winding coils.

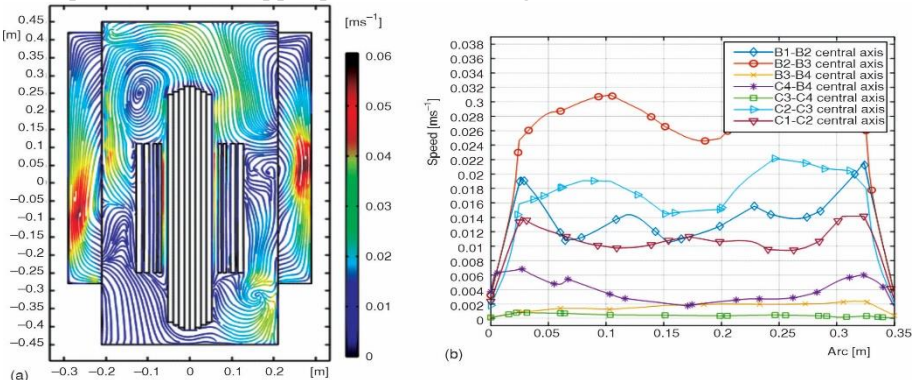

Figure 12. Distribution of transformer fluid field along different paths;
(a) x = 0 plane fluid field distribution and
(b) transformer oil flow velocity along different paths

An improved inversion model of hot spot temperature of oil-immersed transformer based on streamline analysis

Selection of transformer characteristic temperature points based on streamline analysis

The heat transfer mechanism of the oil-immersed transformer has been detailed in section *Solving domain boundary conditions and grid testing*. The transformer oil convective heat transfer in the oil tank transfers the winding heat to the box, and the overall temperature distribution of the transformer is obtained after the final temperature rise is stabilized [18, 19]. The heat dissipation path diagram of the oil flow inside the transformer in the thermal field is shown in fig. 13.

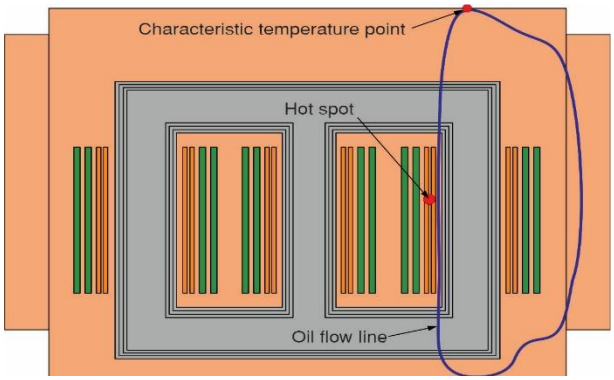

Figure 13. Schematic diagram of heat dissipation of transformer oil flow line

Through the coupling simulation analysis of the transformer fluid-thermal field, the flow lines flowing through the hot spot area and the shell of the transformer are extracted. Considering the structural characteristics and fluid flow characteristics of the transformer, the external characteristic temperature points related to the hot spot temperature are selected, and the non-linear relationship between the characteristic points and the hot spot temperature is constructed to realize the inversion of the transformer hot spot temperature based on the flow line analysis [20]. The selected characteristic temperature points of the transformer are shown in fig. 14.

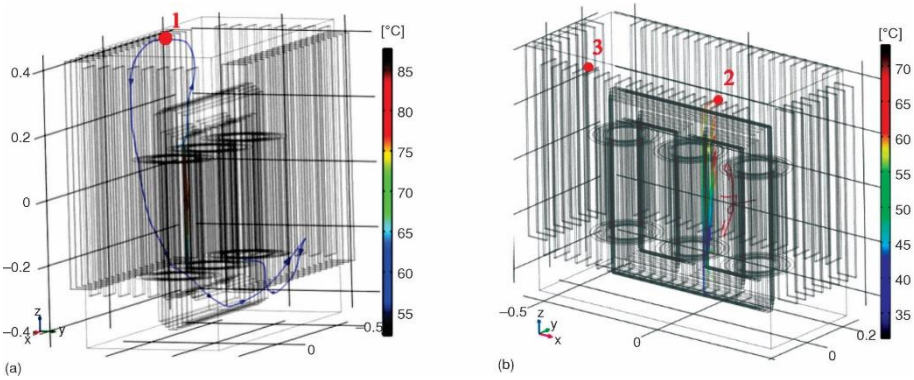

Figure 14. Selection of transformer characteristic temperature points; (a) selection of the characteristic temperature point at the top of the trans-former and (b) selection of the characteristic temperature point of the transformer heat sink

The selected flow lines passing through the transformer hot spot area and the transformer top housing area are shown in fig. 14(a). The cluster curve flows through the B-phase winding region to the top. With the decrease of temperature, the transformer oil density increases and flows back to the bottom of the transformer. Therefore, this point is selected as the characteristic temperature point at the top. Select the flow lines that flow through the transformer winding and heat sink as shown in fig. 14(b). The Point 2 with the highest temperature in the heat sink housing area (the top of the heat sink) is selected as the characteristic temperature point, that is, the entrance of the oil flow in the heat sink. Because of the symmetry of the transformer structure, the characteristic temperature Point 3, which is relative to the characteristic temperature Point 2 near phase C, is selected as the characteristic temperature point.

Additional instructions (Word Style TS Heading 2)

Support vector machine (SVM) is a modeling method based on small sample statistical learning theory and structural risk minimization. The SVM was originally applied in non-linear pattern recognition classification, and with the development of intelligent algorithms, it has shown good performance in non-linear fitting, and has been widely used in transformer fault diagnosis and power system load prediction [21]. In support vector regression, the line needed to fit the data becomes the hyperplane. The basic idea is to find a hyperplane so that the error of all training samples from the hyperplane is minimal, as shown in fig. 15.

Given a training sample S, where x_i represents the i input index, y_i represents its corresponding output vector, and n represents the sample size:

$$S = \{(x_i, y_i), ..., (x_n, y_n)\} \subset R^n \times R \tag{4}$$

The SVM maps the input sample data from the original space to the high-dimensional feature space by seeking a non-linear mapping function, and establishes a linear regression

function in the high-dimensional feature space by using the principle of structural risk minimization, and uses the linear function for linear regression of non-linear problems. The expression of the linear regression function is shown in the equation:

$$y' = w\varphi(x) + b \tag{5}$$

where $\varphi(x)$ is used to describe the high-dimensional feature space H, $w \in H$ – the weight vector, $b \in R$ – the threshold, y' – the predicted value, and y – the measured value.

On the basis of considering the allowable error and introducing the relaxation factors ξ_i and ξ_i^* using the principle of structural risk minimization, the regression problem is transformed into the problem of minimizing the objective function of structural risk, that is, to find the values of w and b that minimize the objective function:

$$\min\left\{\varphi(w) = \frac{1}{2}\|w\|^2 + C\sum_{i=1}^{n}\left(\xi_i + \xi_i^*\right)\right\}$$
$$s.t.\begin{cases} w\varphi(x_i) - y_i + b \le \varepsilon + \xi_i^* \\ y_i - w\varphi(x_i) - b \le \varepsilon + \xi_i \\ \xi_i \ge 0,\ \xi_i^* \ge 0 \end{cases} \tag{6}$$

In this paper, the hot spot temperature of the transformer is taken as the output target. The heat transfer coefficient of the transformer heat sink, *h1*, the heat transfer coefficient of the transformer oil tank wall, *h2*, the ambient temperature, *T*, the winding heat source proportional coefficient, P_i, and the iron core heat source proportional coefficient, P_w, are taken as the factor level based on the simulation model of the transformer fluid-thermal field. The central composite design factors and levels of five factors and five levels established are shown in tab. 3, and the total number of test design samples is 50.

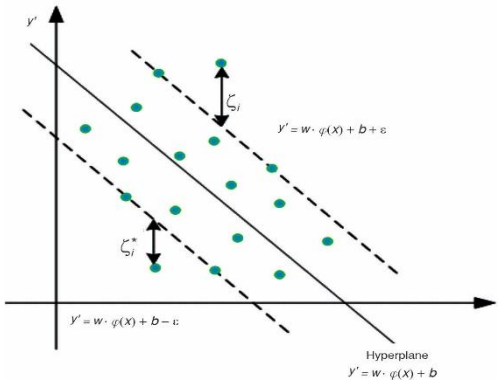

Figure 15. Schematic diagram of support vector regression

Table 3. Central composite design parameters for five factor and five levels

Level of factor	Experimental factor				
	h_1	h_2	T [°C]	P_i	P_w
1	5.00	5.00	10.00	0.80	0.80
2	8.48	8.48	15.80	0.92	0.92
3	11.00	11.00	20.00	1.00	1.00
4	13.52	13.52	24.20	1.08	1.08
5	17.00	17.00	30.00	1.20	1.20

Hot spot temperature inversion results and analysis

The feature point temperature and hot spot temperature based on streamline analysis were extracted from the 50 groups of central composite design experiments aforementioned as sample database, and the hot spot temperature was inverted using SVM algorithm. The training

set and test set are divided according to 70% and 30%, respectively. The pairs of predicted and simulated values of the test set of the hot spot temperature inversion model based on streamline analysis by SVM algorithm are shown in tab. 4, and the error indicators of the inversion model are shown in tab. 5.

Table 4. Comparison between the predicted value and the simulated value of the test set of the predictive model based on streamline analysis

Sample	Artificial value [°C]	Predicted value [°C]	Temperature difference [°C]	Relative error
1	128.7	136.49	7.792	0.061
2	115.16	114.76	0.401	0.003
3	193.44	198.02	4.578	0.024
4	55.8	50.63	5.169	0.093
5	51.8	52.07	0.264	0.005
6	57.84	59.67	1.839	0.032
7	51.8	52.06	0.259	0.005
8	285.67	277.99	7.683	0.027
9	127.33	121.97	5.356	0.042
10	154.65	155.3	0.653	0.004
11	66.54	62.32	4.224	0.063
12	88.96	84.91	4.05	0.046
13	115.15	114.75	0.395	0.003
14	129.1	130.56	1.455	0.011
15	103.79	105.67	1.882	0.018

Table 5. Error indexes of hot spot temperature prediction based on streamline analysis

Error indicator	RMSE	MBE	MAE	R^2
Value	4.002	–0.570	3.067	0.998

According to tab. 4, the relative errors of the hot spot temperature inversion models based on streamline analysis are all within 10%, with the maximum being 0.093, and the errors of 12 groups of test samples are within 5%. The previous data results show that considering the flow line has a positive effect on improving the accuracy of the inversion model of transformer hot spot temperature.

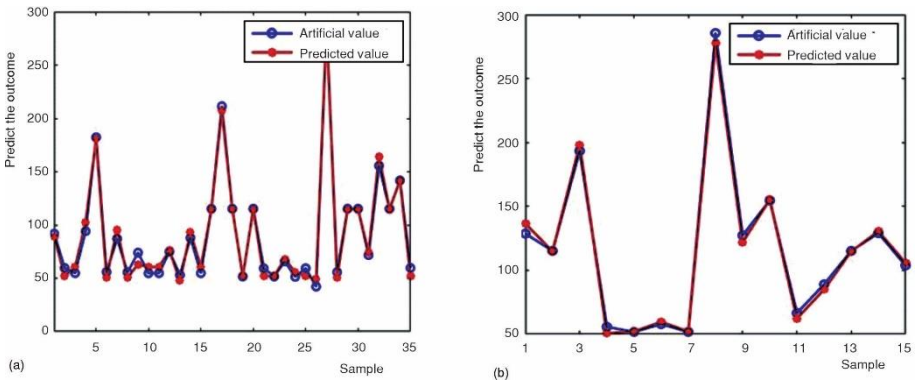

Figure 16. Hot spot temperature prediction results based on streamline analysis; (a) comparison between the training set and the predicted results and (b) comparison between the test set and the predicted results

The predicted value distribution of the hot spot temperature inversion model based on streamline analysis is consistent with the simulated value distribution is shown in fig. 16. The RMSE is 4.002, the average absolute error is 3.067, the average relative error is negative, and the correlation coefficient is 0.998. The prediction accuracy of the model is higher.

Conclusions

Firstly, J-A hysteresis model describing the magnetic properties of materials and its parameter identification. In this paper, the inverse J-A hysteresis model with magnetic induction B as input and magnetization M as output is derived. The PSO was used to solve the parameters of J-A hysteresis model, and the simulation fitting results were compared with the experimental results to verify the accuracy of J-A hysteresis model.

Secondly, aiming at the multi-physical field coupling calculation problem of oil-immersed transformer, considering the characteristics of soft magnetic materials, the distribution law of the transformer's fluid-thermal field is studied by using the bidirectional coupling calculation method of fluid-thermal field. The coil temperature of the axial winding increases first and then decreases, and the highest temperature is about 2/3 of the winding, and the temperature of the low-voltage winding is much higher than that of the high-voltage winding. The temperature distribution law of each phase winding is basically the same, and the temperature of the B-phase winding is slightly higher than that of the C-phase winding. The flow velocity distribution trend at the central axis between different windings is basically the same, showing a phenomenon of fast flow velocity at both ends and slow flow velocity in the middle.

Thirdly, temperature inversion is carried out by support vector regression. The results show that the prediction performance of the model using support vector regression algorithm is slightly reduced when the number of samples is reduced, indicating that the selection of temperature feature points has an impact on the prediction performance. By analyzing the oil flow of the oil-immersed transformer, the characteristic points of the oil tank surface temperature which are strongly correlated with the hot spot temperature are selected. This prediction method has the smallest error and the correlation coefficient is 0.998, which provides an important reference value for the prediction of the hot spot temperature of the transformer.

Acknowledgment

This work is supported by the Open Fund of Beijing Key Laboratory of Distribution Transformer Energy-Saving Technology in 2023 (PDB51202301652).

Nomenclature

a – factor
B – magnetic flux density
b – threshold value
C – penalty factor
c – coefficient of reversibility
H_e – magnetic field strength
k – check coeff. between magnetic domains
M – total magnetization, [Am^{-1}]
M_{rev} – reversible magnetization, [Am^{-1}]
M_s – meter saturation magnetization
M_{irr} – irreversible magnetization, [Am^{-1}]
M_{an} – no hysteresis magnetization, [Am^{-1}]
w – weight vector
x_i – i^{th} input vector
y_i – i^{th} output parameter
y' – predicted value
y – measured value

Greek symbols

α – magnetic domain interaction coefficient
μ_0 – permeability of vacuum, [Am^{-1}]
δ – direction coefficient

References

[1] Liu, L. Q., *et al*., A Fast and Robust Parameter Identification Method of Jiles-Atherton Hysteresis Model for Transformer Core (in Chinese), *High voltage electrical apparatus*, *56* (2020), 01, pp. 55-60
[2] Li, X. P., *et al*., Parameter Identification of Hysteresis Model of Transformer Core (in Chinese), *Power Grid Technology*, *36* (2012), 2, pp. 200-205
[3] Wilson, P. R., *et al*., Optimizing the Jiles-Atherton Model of Hysteresis by a Genetic Algorithm, *IEEE Transactions on Magnetics*, *37* (2001), 2, pp. 989-993
[4] Cao, W., *et al*., Parameter Identification of Current Transformer J-A Model Based on Improved Particle Swarm Optimization (in Chinese), *Electrical Measurement and Instrumentation*, *58* (2021), 5, pp. 70-77
[5] Santisteban, A., *et al*., Numerical Analysis of the Hot-spot Temperature of a Power Transformer with Alternative Dielectric Liquids, *IEEE Trans. on Dielectrics & Elect. Insu.*, *24* (2017), 5, pp. 3226-3235
[6] Wakil, N. E., *et al*., Numerical Study of Heat Transfer and Fluid Flow in a Power Transformer, *International Journal of Thermal Sciences*, *45* (2006), 6, pp. 615-626
[7] Ostrenko, M. V., *et al*., *Power Transformers and Reactors Stay Losses and Temperatures Calculation Using Coupled IEM and FEM Technique*, Computational Technologies in Electrical and Electronics Engineering, Siberia, Russia, 2010
[8] Peker, H. A., *et al*., Solving Steady Heat Transfer Problems via Kashuri Fundo Transform, *Thermal Science*, *26* (2022), 4A, pp. 3011-3017
[9] Peker, H. A., Cuha, F. A., Application of Kashuri Fundo Transform and Homotopy Perturbation Methods to Fractional Heat Transfer and Porous Media Equations, *Thermal Science*, *26* (2022), 4A, pp. 2877-2884
[10] Cuha, F. A., Peker, H. A., Solution of Abel's Integral Equation by Kashuri Fundo Transform, *Thermal Science*, *26* (2022), 4A, pp. 3003-3010
[11] Peker, H. A., Cuha, F. A., Solving One-Dimensional Bratu's Problem via Kashuri Fundo Decomposition Method, *Romanian Journal of Physics*, *68* (2023), 5-6, pp. 1-9
[12] Peker, H. A.,Cuha, F. A., Application of Kashuri Fundo Transform to Decay Problem, *Süleyman Demirel University Journal of Natural and Applied Sciences*, *26* (2022), 3, pp. 546-551
[13] Peker, B., *et al*., Analytical Solution of Newton's Law of Cooling Equation via Kashuri Fundo Transform, *Necmettin Erbakan University Journal of Science and Engineering*, *6* (2024), 1, pp. 10-20
[14] Pan, W. X., *et al*., Hot Spot Temperature Simulation Analysis Method of Oil-immersed Transformer Based on Thermal Field Calculation (in Chinese), On-line first, *Ele. Measurement and Instrumentation*, 2022
[15] Kennedy, J., Eberhart, R., Particle Swarm Optimization, *Proceedings*, IEEE International Conference on Neural Networks Piscataway, New Jersey, USA, 1995, pp. 1942-1948
[16] Zhang, X. H., *et al*., Parameter Identification of Power Line Communication Multipath Transmission Model Based on Improved Particle Swarm Optimization Algorithm (in Chinese), *Grid technology*, *33* (2009), 1, pp.75-79
[17] Tang, Z., *et al*., Simulation and Analysis of Thermal Network Model of Dry-type Transformer Considering Fluid Dynamics (in Chinese), *Transactions of China Electrotech. Society*, *37* (2022), 18, pp.4777-4787
[18] Tu, W. M., *et al*., Internal Fluid Field Simulation and On-line Fault Prediction Method of Oil-immersed Transformer (in Chinese), *Power Grid Technology*, *34* (2010), 5, pp. 195-200
[19] Yuan, F. T., et al., Temperature Characteristic Analysis and Radiator Optimization of Oil-immersed Transformer Based on Multiphysics Simulation (in Chinese), *High Voltage Eng.*, 51 (2023), 1, pp. 221-231
[20] Deng, Y. Q., *et al*., Establishment and Verification of a Hot Spot Temperature Inversion Model for 10kV Oil-immersed Transformer Windings Based on Streamline Analysis (in Chinese), *Chinese Journal of Electrical Engineering*, *43* (2023), 08, pp. 3191-3204
[21] Ni, J., *et al*., An Adaptive Approach Based on KPCA and SVM for Real-time Fault Diagnosis of HVCBs, *IEEE Transactions on Power Delivery*, *26* (2011), 3, pp.1960-1971

Paper submitted: March 30, 2024
Paper revised: May 18, 2024
Paper accepted: May 23, 2024